ELSEVIER

Journal of Alloys and Compounds 460 (2008) 426–431

Journal of ALLOYS AND COMPOUNDS

www.elsevier.com/locate/jallcom

Crystal structure analysis and thermoelectric properties of p-type pseudo-binary $(Al_2Te_3)_x$–$(Bi_{0.5}Sb_{1.5}Te_3)_{1-x}$ $(x = 0 \sim 0.2)$ alloys prepared by spark plasma sintering

J.L. Cui [a,*], H.F. Xue [a,b], W.J. Xiu [a,b], L.D. Mao [a,c], P.Z. Ying [b], L. Jiang [b]

[a] *School of Mechanical Engineering, Ningbo University of Technology, Ningbo 315016, China*
[b] *School of Materials Science and Engineering, China University of Mining and Technology, Xuzhou 221008, China*
[c] *College of Chemical Engineering and Materials Science, Zhejiang University of Technology, Hangzhou 310014, China*

Received 20 February 2007; received in revised form 16 May 2007; accepted 17 May 2007
Available online 21 May 2007

Abstract

p-Type pseudo-binary alloys $(Al_2Te_3)_x$–$(Bi_{0.5}Sb_{1.5}Te_3)_{1-x}$ $(x = 0 \sim 0.2)$ were prepared by spark plasma sintering (SPS) technique and their thermoelectric properties were evaluated. Measurements show that the Seebeck coefficient decreases and electrical conductivity increases with Al_2Te_3 content increasing due to a possible increment of free carrier (holes) concentration and establishment of special conducting mechanism upon adding Al_2Te_3. Thermal conductivity (κ) increases with temperature but reduces noticeably over the broad temperature range, such a reduction is directly attributed to the enhancement of phonon scattering resulted from both the precipitation of the second phase AlSb and nearly 12% atomic occupation of element Al in Te1 and Te2 sites in the crystal. The maximum ZT value of 0.86 can be obtained for $x = 0.1$ at 419 K, which is 0.28 higher than that of $Bi_{0.5}Sb_{1.5}Te_3$ under the same fabrication technology.

Keywords: Thermoelectric property; Spark plasma sintering; p-Type pseudo-binary $(Al_2Te_3)_x$–$(Bi_{0.5}Sb_{1.5}Te_3)_{1-x}$ alloys

1. Introduction

Bi–Te based alloy $Bi_{0.5}Sb_{1.5}Te_3$ is one of the best p-type thermoelectric materials used in room temperatures. For the application of Bi–Te or Bi–Sb based alloys it is necessary to prepare single or polycrystalline materials with well defined physical parameters (Seebeck coefficient, electrical and thermal conductivity, mobility of free carriers) that can be modified by doping suitable foreign atoms. Such researches as the incorporations of Ag and Ti in the crystal lattice of Bi_2Sb_3 [1–3] that can noticeably influence the transport properties and concentration holes, and as doping of Cu in the $GeBi_4Te_7$ or Tl in the (Bi, Sb)–Te alloys that can substantially reduce the lattice thermal conductivity and electron mobility [4–6]. Since the multi-element compounds can exhibit some unique characteristics such as non-uniform distribution of Sb atoms and isoelectronic substitution between metal ions in the lattice in the K–Bi–Sb–Se and Ag–Pb–Sb–Te thermoelectric alloys [7,8], and introductions of compounds into the Bi_2Te_3 to form nATe.$m$$Bi_2Te_3$ (A = Ge, Sn, Te) [9] evidenced the potential importance for thermoelectric applications, supposing that these introductions can increase the crystal defects through lattice disorder or alteration of crystal constant of cells. Therefore, there is a growing interest in developing the materials with complex structures.

The results from recent research in our group also confirmed that proper introductions of Ag, Cu and Ga [10–12] in the $Bi_{0.5}Sb_{1.5}Te_3$ alloy are essential in improving the thermoelectric performance, due to their substantial enhancement of electrical conductivity and reduction of lattice thermal conductivity, without noticeable loss of Seebeck coefficient. An addition of compound as $Ag_{0.365}Sb_{0.558}Te$ into the Bi–Te based

* Corresponding author. Tel.: +86 574 87081258; fax: +86 574 87081258.
E-mail address: cuijl@nbip.net (J.L. Cui).

0925-8388/$ – see front matter © 2007 Elsevier B.V. All rights reserved.
doi:10.1016/j.jallcom.2007.05.063

alloys is a new approach to modulate the thermoelectric properties in question [13], the compound $Ag_{0.365}Sb_{0.558}Te$ with cubic type (sp.gr. *Fm-3m*) can possibly combine Sb_2Te_3 or Bi_2Te_3 slabs to form a special alloy favoring carrier transportation. Again, Al_2Te_3 is a compound with a ZnS structure (sp.gr. $P6_3\,mc$), if Al_2Te_3 substitutes for $Bi_{0.5}Sb_{1.5}Te_3$, many vacancies can also be introduced. This special alloy can be expected to behave similar performance to that of $Ag_{0.365}Sb_{0.558}Te$, being beneficial to the optimization of free carrier concentration (holes), causing an improvement of thermoelectric properties. On the other hand, although the atomic radius of Al (1.82×10^{-10} m) shares almost the same value as that of Ga (1.81×10^{-10} m), the elelctronegativity of Al (1.61) is smaller than that of Ag (1.93) [14], which might enable Al_2Te_3-doped $(Al_2Te_3)_x$–$(Bi_{0.5}Sb_{1.5}Te_3)_{1-x}$ alloys to have a larger product of effective mass and mobility of carriers than $Ag_{0.365}Sb_{0.558}Te$-doped $(Ag_{0.365}Sb_{0.558}Te)_x$–$(Bi_{0.5}Sb_{1.5}Te_3)_{1-x}$ alloys.

In the present paper, structural refinement for the powders of $(Al_2Te_3)_x$–$(Bi_{0.5}Sb_{1.5}Te_3)_{1-x}$ crystals was carried out and the samples are characterized by measurements of the temperature dependence of Seebeck coefficient, electrical conductivity, and thermal conductivity in the temperature range of 319–534 K, with the aim to investigate how these quantities are affected by the introduction of Al_2Te_3 into the crystals of $(Al_2Te_3)_x$–$(Bi_{0.5}Sb_{1.5}Te_3)_{1-x}$.

2. Experimental

Two mixtures of Al_2Te_3 and $Bi_{0.5}Sb_{1.5}Te_3$ were weighted from the elements of Al, Bi, Sb, Te with 5 N purity, and sealed in two different evacuated quartz tubes, the subsequent melting was conducted for 10 h at 1373 K, and then quenching in water. Since Al_2Te_3 is not stable in air, after weighing of Al_2Te_3 and $Bi_{0.5}Sb_{1.5}Te_3$ ingots according to stoichiometry of $(Al_2Te_3)_x$–$(Bi_{0.5}Sb_{1.5}Te_3)_{1-x}$ ($x = 0$, 0.05, 0.1, 0.2), quick evacuation and sealing for the mixtures by two ingots is strongly required, and subsequent melting and quenching processes were repeated. During all melting 30-s rocking every 1 h was conducted to ensure that the composition was homogenous without segregation, obtained $(Al_2Te_3)_x$–$(Bi_{0.5}Sb_{1.5}Te_3)_{1-x}$ ingots with different molar fraction x were ball-milled in stainless steel bowls for 5 h with a rotation rate of 350 rpm. Prior to sintering, the powders were dried in vacuum for 5 h at 60 °C, the sintering was carried out using a spark plasma sintering apparatus (SPS-1030) at a pressure of 40 Mpa, the densities of the sintered samples were measured using an Archimedes method. Finally, each sample was cut into 3 mm slices measuring 2.5 mm × 15 mm from the sintered block with the size of ϕ 20 mm × 2.5 mm for property measurement.

The crystal structure was analyzed at room temperature with X-ray diffractometer (XRD-98) using Cu Kα radiation ($\lambda = 0.15406$ nm), using a scan rate of 4° min^{-1} to record the patterns in the 2θ range from 10 to 110°. Lattice constants, the quantity of second phases and the occupation percent of atoms in the sublattices were examined using Rietveld refinement. An EPMA was performed to examine the compositions for all the starting materials using Electron Probe Microanalysis (EPMA-8705QH2) with an accuracy of more than ±97%. The morphologies of the polished samples were observed by a back-scattered electron image (BSEI) (JXA-8100) and the compositions in different areas for the sample with $x = 0.2$ were evaluated.

The transport properties involving Seebeck coefficients (α) and electrical conductivities (σ) were measured using an apparatus (ULVAC ZEM-2) in a helium atmosphere. Thermal diffusivities were measured by a laser flash method (Netzsch, LFA427), and thermal conductivities were calculated from the values of densities, specific heats and thermal diffusivities.

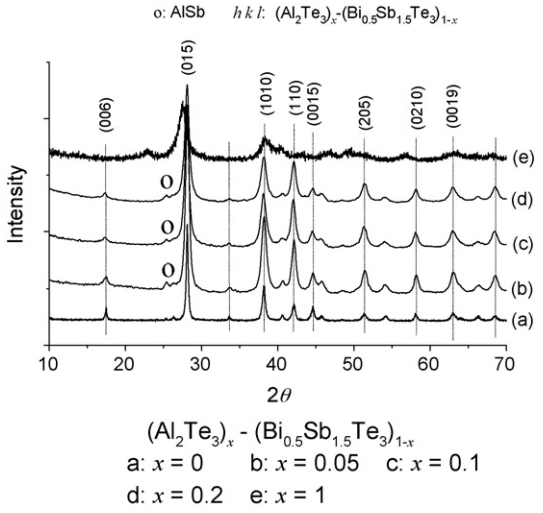

Fig. 1. X-ray diffraction patterns of the $(Al_2Te_3)_x$–$(Bi_{0.5}Sb_{1.5}Te_3)_{1-x}$ ($x = 0 \sim 1$) alloys, (a) $x = 0$; (b) $x = 0.05$; (c) $x = 0.1$; (d) $x = 0.2$; (e) $x = 1$.

3. Results and discussion

3.1. Rietveld analysis of X-ray diffraction profiles and evaluation of chemical compositions

The X-ray diffraction patterns of the samples are shown in Fig. 1, the patterns for Al_2Te_3 and $Bi_{0.5}Sb_{1.5}Te_3$ are specially displayed for comparison. It is confirmed that the majority phase is found to be $(Al_2Te_3)_x$–$(Bi_{0.5}Sb_{1.5}Te_3)_{1-x}$ with rhombohedral lattice structure as $Bi_{0.5}Sb_{1.5}Te_3$ (sp.gr. $R\bar{3}m$), the intensity peaks of the main planes as (0 0 6), (1 0 1 0), (1 1 0), (0 0 1 5), (2 0 5) and so on obviously increases after introduction of Al_2Te_3. Since the melting point of AlSb is 1331 K, much higher than those of any other compounds, hence it is explainable that a small amount of second phase AlSb can precipitate during cooling, its quantities are shown in Table 1.

Table 1
Analyzed lattice parameters and the second phase of $(Al_2Te_3)_x$–$(Bi_{0.5}Sb_{1.5}Te_3)_{1-x}$ by Rietveld analysis of the powder XRD profiles

Sample with x	$(Al_2Te_3)_x$–$(Bi_{0.5}Sb_{1.5}Te_3)_{1-x}$			
Lattice parameters and foreign phase	$x = 0$	$x = 0.05$	$x = 0.1$	$x = 0.2$
a (nm) (analyzed)	0.4297	0.4291	0.4290	0.4288
c (nm) (analyzed)	3.0517	0.3044	0.3045	0.3047
AlSb (wt.%) (analyzed)		1.5	2.2	2.2
Occupation percent of Al at Te1 site (%)		15.5	14.2	8.65
Occupation percent of Al at Te2 site (%)		10.3	9.06	14.5

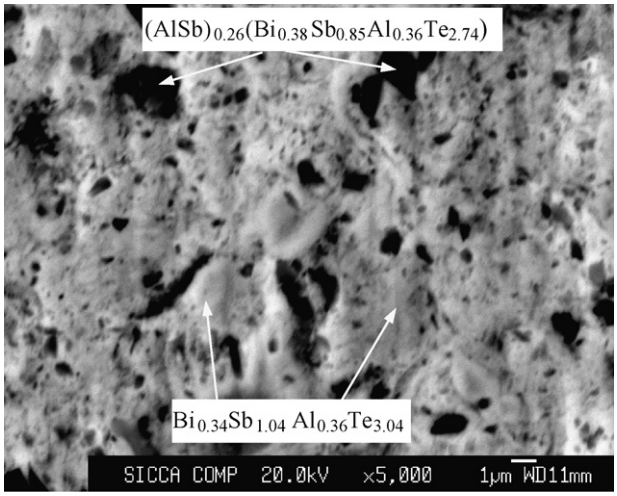

Fig. 2. The back-scattered electron image (BSEI) of Al_2Te_3-doped $(Al_2Te_3)_x$–$(Bi_{0.5}Sb_{1.5}Te_3)_{1-x}$ alloy with $x = 0.2$ using JXA-8100.

Structural refinement reveals that a certain amount of Al atoms are in the main phase with Te1 and Te2 sites occupied with Al atoms respectively, an occupation percent of Al at Te1 site gradually decreases from 15.5 to 8.65%, while that at Te2 generally increases from 10.3 to 14.5% with Al_2Te_3 content increasing, an average occupation percent of Al is about 12% for the materials in question. The lattice constants a becomes smaller and c becomes larger with Al_2Te_3 content increasing, shown in Table 1. This might be caused by the smaller radius of Al than that of Te and possible intercalation of the second phase AlSb in the main crystals. Through the observation for the sample with $x = 0.2$ using back-scattered electron image, the morphologies presented in Fig. 2 indicate that black area is Al-rich compound with the composition being $Al_{0.62}Bi_{0.38}Sb_{1.21}Te_{2.74}$, which can be estimated to be the formula as $(AlSb)_{0.26}(Bi_{0.38}Sb_{0.85}Al_{0.36}Te_{2.74})$, based on the calculation of occupation percent of Al atoms (~12%) in Te1 and Te2 sites, shown in Table 2. White area is Al-poor compound with the composition being $Bi_{0.34}Sb_{1.04}Al_{0.36}Te_{3.04}$ almost without formation of AlSb phase. According to these estimated compositions, it is easy to figure out that the quantity of AlSb precipitated, shown in Table 1, is a little lower than that from the calculation in the $(AlSb)_{0.26}(Bi_{0.38}Sb_{0.85}Al_{0.36}Te_{2.74})$ in black areas (Fig. 2). Therefore, we can presume that some AlSb might be intercalated in the main phase of $(Al_2Te_3)_x$–$(Bi_{0.5}Sb_{1.5}Te_3)_{1-x}$, resulting in gradual increment of constant c.

The content of Al was analyzed using EPMA for the powders of $(Al_2Te_3)_x$–$(Bi_{0.5}Sb_{1.5}Te_3)_{1-x}$, we find that the content of Al increases with molar fraction x, while those of Bi and Sb gradually decrease, shown in Table 3, being in very well agreement with those of the starting compositions.

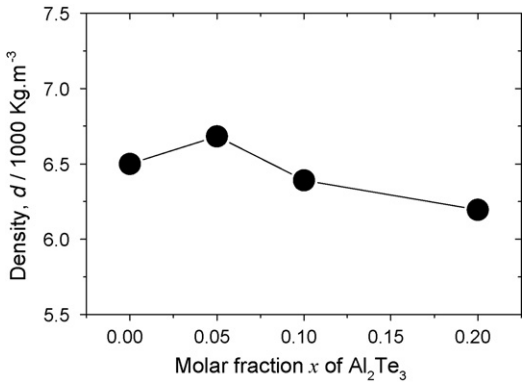

Fig. 3. The relationship between density and molar fraction x of Al_2Te_3 for the alloys $(Al_2Te_3)_x$–$(Bi_{0.5}Sb_{1.5}Te_3)_{1-x}$ ($x = 0 \sim 0.2$) prepared by spark plasma sintering.

The densities of the alloys, measured using Archimedes method, are shown in Fig. 3, where the density increases with Al_2Te_3 content up to $x = 0.05$, and then decreases. The maximum density is 6.68×10^3 kg/m^3, and the relative densities are higher than 93.0% for all the $(Al_2Te_3)_x$–$(Bi_{0.5}Sb_{1.5}Te_3)_{1-x}$ alloys. In general, the changes of density under introduction of Al_2Te_3 depend both on the masses of the substituted and substituting atoms and on the changes in unit cell parameters. The possible explanation for the densification with limited introduction of Al_2Te_3 ($x = 0.05$) might be due to the fact that the precipitated second phase AlSb plays a role as a sintering accelerator, a proper segregated second phase AlSb distributed in the grain boundaries can suppress grain growth, hence the pores in the sintered structure can partially be eliminated. When $x > 0.05$, a reduction of density is considered to be caused by the density difference between substituting and substituted compounds of Al_2Te_3 (4.5×10^3 kg/m^3) and $Bi_{0.5}Sb_{1.5}Te_3Te$ (6.858×10^3 kg/m^3).

3.2. Thermoelectric properties

The temperature dependence of the Seebeck coefficient (α) for the $(Al_2Te_3)_x$–$(Bi_{0.5}Sb_{1.5}Te_3)_{1-x}$ alloys is shown in Fig. 4. The measured α values are positive, indicating p-type semiconductor behavior. The α values for the Al_2Te_3-doped alloys generally decrease with Al_2Te_3 content increasing, suggesting that the doping of Al_2Te_3 in the $Bi_{0.5}Sb_{1.5}Te_3$ alloy can result in an increment of carrier (holes) concentration. The maximum α value of 194.7 (μV/K) appears at about 419 K when $x = 0.1$. When at high temperatures above 419 K, the α values are gradually approaching each other and going to be higher than those of the alloy without doping. The slope of the Seebeck coefficients has greatly changed upon adding Al_2Te_3, which might pertain to substantial electronic changes at a Fermi level. On the other hand, when assuming a Boltzmann distribution for the

Table 2
The average chemical compositions (wt.%) in different areas for the sample with $x = 0.2$ (three different spots were taken while analyzing)

Area	Al	Bi	Sb	Te	Estimated compositions
Black area	2.90	13.91	25.45	57.74	$(AlSb)_{0.26}(Bi_{0.38}Sb_{0.85}Al_{0.36}Te_{2.74})$
White area	0.61	12.39	22.17	64.83	$Bi_{0.34}Sb_{1.04}Al_{0.36}Te_{3.04}$

Table 3
Average molar fraction of elements in the alloys $(Al_2Te_3)_x$-$(Bi_{0.5}Sb_{1.5}Te_3)_{1-x}$ analyzed by EMPA (four different points were taken when analyzed)

Samples with x	Molar fraction of elements			
Element	$x=0$	$x=0.05$	$x=0.10$	$x=0.20$
Al		0.062	0.186	0.379
Sb	1.5290	1.386	1.289	1.098
Te	2.9630	2.979	2.968	2.976
Bi	0.4540	0.436	0.422	0.386
Remaining elements		Oxygen		

holes, the relationship between Seebeck coefficient α at a given temperature is given by [15]:

$$\alpha = \frac{\kappa_B}{e}\left[s + \frac{5}{2} + \ln\frac{2(2\pi m^* \kappa_B T)^{3/2}}{nh^3}\right] \quad (1)$$

where κ_B is the Boltzmann constant; e the electronic charge; m^* effective mass; n the carrier concentration; h Planck's constant; s, the scattering parameter. According to the above equation, an increase of scattering factor s especially at higher temperatures is obviously due to the increased carrier scatterings in the grain boundaries from the precipitation of AlSb and point defects resulted from Al occupation in the Te1 and Te2 sites, which enables α values to increase almost linearly with s, despite the fact that an increment of carrier (holes) concentration can reduce the α values. The final outcome is that the α values decrease mildly and approach each other at elevated temperatures.

The relationship between the electrical conductivity (σ) and temperature is shown in Fig. 5. The σ value gradually increases with Al_2Te_3 content, and decreases from 5.1×10^4 to 3.6×10^4 $\Omega^{-1}\,m^{-1}$ with temperature rising from 319 to 534 K for $x = 0.1$. These σ values are approximate 2.8 and 1.4 times those of the ternary alloy $Bi_{0.5}Sb_{1.5}Te_3$, suggesting that the carriers are in an extrinsic state in the whole temperature range, and the Al_2Te_3-doped $(Al_2Te_3)_{1-x}$–$(Bi_{0.5}Sb_{1.5}Te_3)_x$ alloys have a larger carrier concentration (holes), product of effective mass and mobility of carriers. Another explanation to the improvement of σ might be the fact that there is another mechanism of carrier transportation after doping of Al_2Te_3 into $Bi_{0.5}Sb_{1.5}Te_3$. Since a certain amount of Te1 and Te2 sites are occupied with Al atoms in the crystals, a special electron transportation mechanism might be established, favoring the improvement of electrical conductivity.

The total thermal conductivity (κ) can be expressed by the sum of a lattice (κ_L), electronic ($\kappa_{carrier}$) and ambipolar (κ_{am}) component, i.e., $\kappa = \kappa_L + \kappa_{carrier} + \kappa_{am}$, $\kappa_{carrier}$ can be estimated from Wiedemann–Franz's law as $\kappa_{carrier} = LT\sigma$, where L is the Lorenz number ($L = 1.5 \times 10^{-8}\,V^2\,K^{-2}$) for a degenerate semiconductor [16]. The temperature dependence of κ value is indicated in Fig. 6(a), where one can find that the κ value increases with measuring temperature for all alloys, ranging from 0.72 to 1.06 $W\,K^{-1}\,m^{-1}$ for $x = 0.1$ when temperature is elevated from 319 to 534 K. With an increase of molar fraction x the κ value decreases at the corresponding temperatures. Since the electronic component $\kappa_{carrier}$ is strongly dependent on the σ value, a rising $\kappa_{carrier}$ value with Al_2Te_3 content can be expected, shown in Fig. 6(b). Therefore, the reduction of total κ value with x is largely attributed to the reduction of κ–$\kappa_{carrier}$ with the increasing of Al_2Te_3 content shown in Fig. 6(c). Noting that the κ–$\kappa_{carrier}$ value keeps almost constant for all the

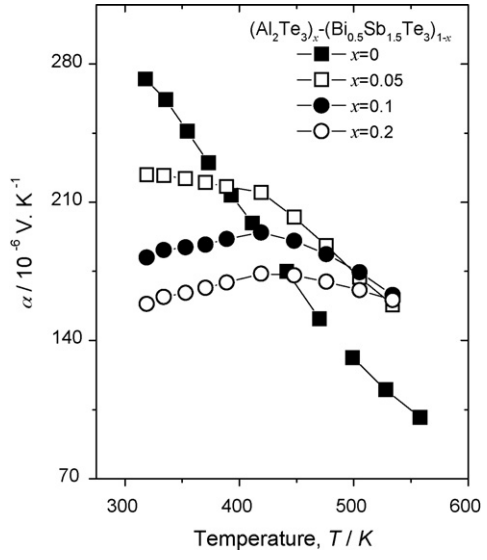

Fig. 4. The relationship between temperature and Seebeck coefficients for different $(Al_2Te_3)_x$–$(Bi_{0.5}Sb_{1.5}Te_3)_{1-x}$ ($x = 0 \sim 0.2$) alloys prepared by spark plasma sintering.

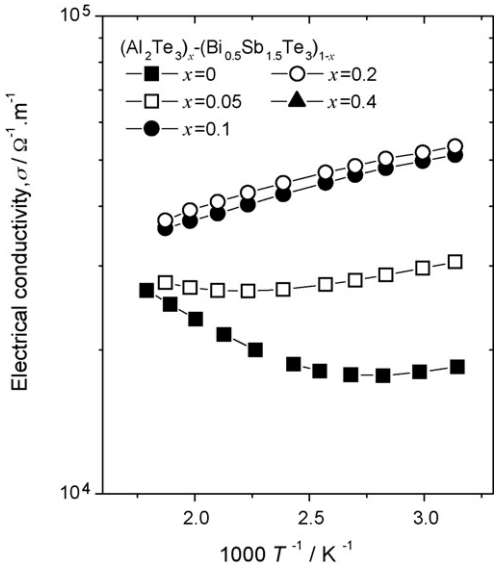

Fig. 5. The dependence of electrical conductivities on temperature for different $(Al_2Te_3)_x$–$(Bi_{0.5}Sb_{1.5}Te_3)_{1-x}$ ($x = 0 \sim 0.2$) alloys prepared by spark plasma sintering.

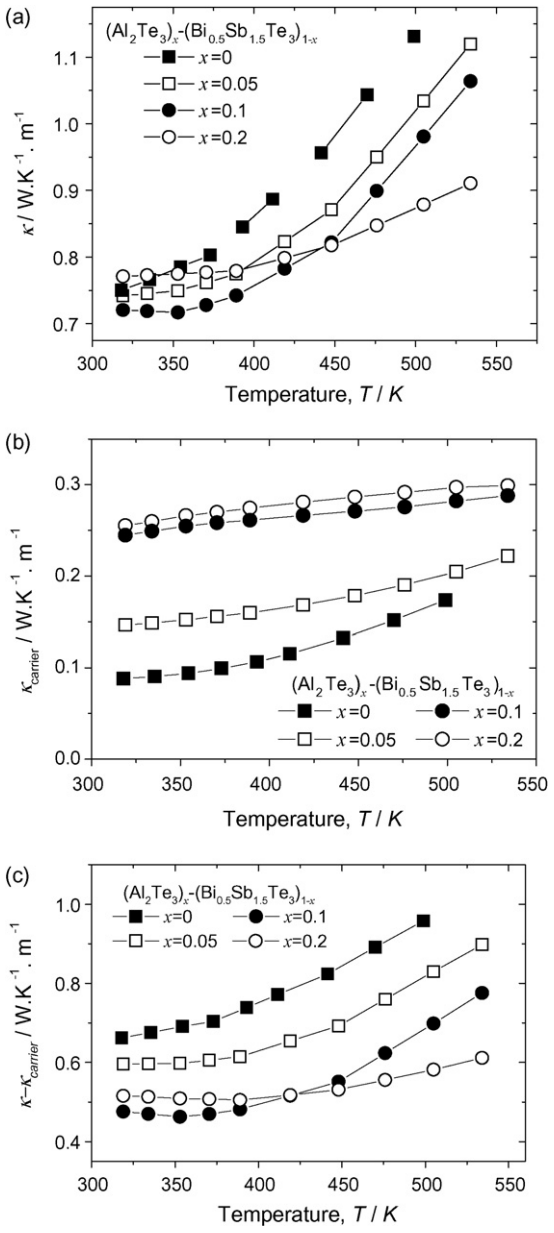

Fig. 6. The temperature dependence of thermal conductivities for different $(Al_2Te_3)_x$–$(Bi_{0.5}Sb_{1.5}Te_3)_{1-x}$ ($x = 0 \sim 0.2$) alloys prepared by spark plasma sintering, (a) κ–T, (b) $\kappa_{carrier}$–T, (c) κ–$\kappa_{carrier}$–T.

Al_2Te_3 doped alloys below 419 K, and above that it rises relatively rapidly. This apparent increase of κ–$\kappa_{carrier}$ values might directly be caused by ambipolar contribution arising from the diffusion of electron-hole pairs with the onset of intrinsic contribution that is apparently indicated in the α–T curves, shown in Fig. 4. On the other hand, however, although a rising trend of κ–$\kappa_{carrier}$ value with temperature is obtained for all the doped alloys, for the alloy with $x = 0.2$ relatively low but a mild increment of κ–$\kappa_{carrier}$ value above 419 K can be observed. This suggests that the gradual enhancement of phonon scattering, both in the grain boundaries due to the precipitation of AlSb and point defects from the occupation of Al in the Te1 and Te2 sites, can be observed with Al_2Te_3 content increasing, the more the Al_2Te_3 content, the more the grain boundaries (Fig. 2).

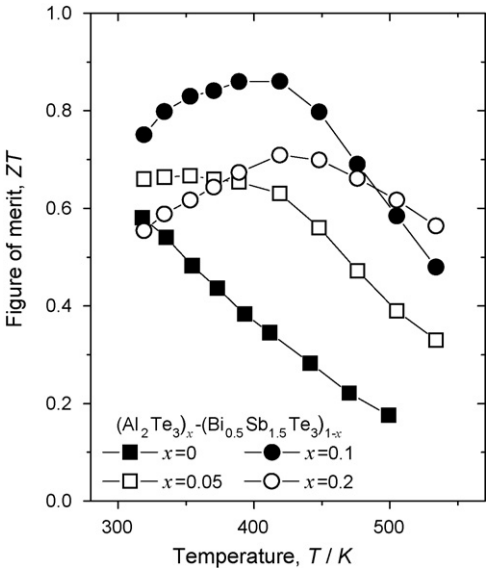

Fig. 7. The temperature dependence of dimensionless thermoelectric figure of merit ZT for different $(Al_2Te_3)_x$–$(Bi_{0.5}Sb_{1.5}Te_3)_{1-x}$ ($x = 0 \sim 0.2$) alloys prepared by spark plasma sintering.

The ZT value against temperature is plotted in Fig. 7. With an increase of Al_2Te_3 content the maximum ZT value gradually shifts to the higher temperature side and increases up to $x = 0.1$. An optimal ZT value of 0.86 is obtained for $x = 0.1$ at 419 K, this value is 0.28 higher than that of the ternary alloy $Bi_{0.5}Sb_{1.5}Te_3$. Since the thermoelectric figure of merit ZT of about 1 for Bi–Te based alloys can usually be obtained near room temperature [17–20], therefore, if proper fabrication technique were employed in the present material systems, much higher thermoelectric performance would be expected than the observed alloys here simply fabricated by powder metallurgy. Using the present fabrication technique the sample of Al_2Te_3 is very hard to prepare due to its strong brittleness and unstable in air, hence we could not so far evaluate its thermoelectric properties, which makes it difficult to directly compare the thermoelectric properties with those of the pseudo-binary alloys.

4. Conclusions

The samples of $(Al_2Te_3)_x$–$(Bi_{0.5}Sb_{1.5}Te_3)_{1-x}$ ($x = 0 \sim 0.2$) were prepared by spark plasma sintering (SPS) technique and their physical properties were evaluated. The thermoelectric properties can obviously be improved upon adding Al_2Te_3 with the maximum ZT value of 0.86 obtained at 419 K for $x = 0.1$, which is 0.28 higher than that of $Bi_{0.5}Sb_{1.5}Te_3$. The Seebeck coefficient decreases and electrical conductivity increases with an increase of Al_2Te_3 content, due to the possible increment of free carriers (holes) and establishment of special conducting mechanism. A substantial reduction of thermal conductivity upon adding Al_2Te_3 is directly attributed to the enhancement of phonon scattering in the grain boundaries due to the precipitation of AlSb and distorted lattices from the occupation of Al in the Te1 and Te2 sites.

Acknowledgements

The Project supported by the Link Project with Israel (ALIS) in 2007, and Ningbo Natural Science Foundation of China (No. 2006A610058).

References

[1] P. Lošt'ák, Č. Drašar, J. Horák, Z. Zhou, J.S. Dyck, C. Uher, J. Phys. Chem. Solids 67 (2006) 1457–1463.
[2] Č. Drašar, M. Steinhart, P. Lošt'ák, H.-K. Shin, J.S. Dyck, C. Uher, J. Solid State Chem. 178 (2005) 1301–1307.
[3] J. Navrátil, I. Klichová, S. Karamazov, J. Šrámková, J. Horák, J. Solid State Chem. 140 (1998) 29–37.
[4] L.E. Shelimova, O.G. Karpinskii, P.P. Konstantinov, M.A. Kretova, E.S. Avilov, V.S. Zemskov, Inorg. Mater. 38 (2002) 790–794.
[5] K. Kurosaki, H. Uneda, H. Muta, S. Yamanaka, J. Alloys Compd. 376 (2004) 43–48.
[6] S. Yamanaka, A. Kosuga, K. Kurosaki, J. Alloys Compd. 352 (2003) 275–278.
[7] T. Kyratsi, D.-Y. Chung, M.G. Kanatzidis, J. Alloys Compd. 338 (2002) 36–42.
[8] K.F. Hsu, S. Loo, F. Guo, W. Chen, J.S. Dyck, C. Uher, T. Hogen, E.K. Polychroniadis, M.G. Kanatzidis, Science 303 (2004) 818–821.
[9] L.E. Shelimova, P.P. Konstantinov, O.G. Karpinskii, E.S. Avilov, M.A. Kretova, V.S. Zemskov, J. Alloys Comp. 329 (2001) 50–62.
[10] J.L. Cui, H.F. Xue, W.J. Xiu, Mater. Lett. 60 (2006) 3669–3672.
[11] J.L. Cui, H.F. Xue, W.J. Xiu, W. Yang, X.B. Xu, Scripta Mater. 55 (2006) 371–374.
[12] J.L. Cui, H.F. Xue, W.J. Xiu, Mater. Sci. Eng. (B) 135 (2006) 44–49.
[13] J.L. Cui, H.F. Xue, W.J. Xiu, J. Solid State. Chem. 179 (2006) 3751–3755.
[14] M.L. Li, Concise Handbook of Chemical Data (in Chinese), Chemical Engineering Press, Beijing, 2003, pp. 6.
[15] S.S. Kim, S. Yamamoto, T. Aizawa, J. Alloys Comp. 375 (2004) 107–113.
[16] R. Venkatasubramanian, E. Siivola, T. Colpitts, B. O'Quinn, Nature 413 (2001) 597–602.
[17] N.T. Huong, Y. Setou, G. Nakamoto, M. Kurisu, T. Kajihara, H. Mizukami, S. Sano, J. Alloys Comp. 368 (2004) 44–50.
[18] J. Seo, D. Cho, K. Park, C. Lee, Mater. Res. Bull. 35 (2000) 2157–2163.
[19] T.S. Kim, B.S. Chun, J. Alloys Comp. 437 (2007) 225–230.
[20] T.S. Kim, B.S. Chun, J.K. Lee, H.G. Jung, J. Alloys Comp. 434–435 (2007) 710–713.